ENERGY HARVESTING BETWEEN UAVS FOR BACKHAUL CONNECTION

Le Tung Hoa, Nguyen Van Thang, Dang The Ngoc
Wireless Systems and Applications Laboratory
Posts and Telecommunications Institute of Technology

Abstract— UAV (Unmanned Aerial Vehicle) has become an essential part of 6G. UAVs can make it easier to have a LOS (light-of-sight) connection and quicker to launch a network. However, backhaul connection and energy limitations are two main reasons that slow down UAV usage. In our research, we propose a mixture model, which combines a tethered UAV and a UAV. The tethered UAV is connected to a truck by a fiber optic cable that ensures energy and fast data transmission to it via optical communication. The tethered UAV forwards laser signals from the truck to the UAV to charge and transfer data simultaneously via FSO (free space optical) communication. We consider the harvested energy collected at the UAV under a given BER (bit error rate). The harvested energy is evaluated by multiple factors, such as transmitted power, the position of the UAV, and the FSO link length in our simulation results. The FSO link includes several phenomena, such as atmospheric attenuation, turbulence, and pointing error.

Keywords—energy harvesting, UAV, tethered UAV, FSO communications.

I. INTRODUCTION

The astounding development of technology has changed all aspects of our lives. The continuous born of many mobile network generations from 2G to 4G has proven significantly how much information traffic people have needed to share. Nevertheless, the percentage of all people having the ability to utilize all those advanced networks is surprisingly limited, only around 50%. Due to an ITU publication [1], by the end of 2021, three billion people were inaccessible to the Internet and many modern applications. Recently, we have reached the next era of mobile networks, the so-called Beyond 5G (B5G) or 6G. Some of the main targets of 6G are to provide worldwide and continuous connectivity. The worldwide purpose targets a few challenging areas that are hard to reach from previous network generations, such as rural areas, spare places, and isolated islands. The continuous connectivity aims to implement a quick network after some critical natural disasters. Those purposes have been realistic by the meaningful support of UAVs. Since releases 15, 16, and 17, 3GPP has provided some specifications to attach UAVs to the existing cellular networks [2].

Contact author: Nguyen Van Thang
Email: thangnv@ptit.edu.vn
Manuscript received: 8/2022, revised: 9/2022, accepted: 10/2022.

UAVs have become more and more popular in networks due to their two main advantages, the better channel quality of LOS and quicker network launch. These advantages have made UAVs one of the essential factors in 6G [3-4]. However, UAV usage remains with some problems of energy limitation and backhaul connection. Thanks to the new type of UAV, tethered UAVs, they have been solved more easily.

Tethered UAVs are UAVs tethered to a ground unit. The clever idea of leasing UAVs has lifted many obstacles which untethered UAVs always face. Firstly, tether cables can provide seemingly unlimited power to UAVs. It guarantees seamless connection and increases their endurance and persistence. Secondly, tether cables make it possible to support ultra-high-speed data. So, tethered UAVs can be used for backhaul connections with high data rate requirements. The only limitation of tethered UAVs is mobility compared with untethered UAVs [5].

Untethered UAVs are more flexible in deciding their flying paths than tethered UAVs. If we need to make more dynamic and flexible networks, untethered UAVs must be used. In our research, we have thought about a network combining both types, untethered and tethered UAVs. We have tried to take advantage of both types and leverage the whole network. The tethered UAV delivers a backhaul connection with unlimited power and then transfers signals to another untethered UAV with better mobility. However, the link between tethered and untethered UAVs is not only for data transmission purposes but also for wirelessly charging the UAV through FSO communication, which is called energy harvesting. FSO communication is used between tethered and untethered UAVs because it can support high data transmission, like an optical fiber, and has a laser beam with higher energy concentration to enable a better charge [6]. The tethered UAV will simultaneously transfer data information and charge to the untethered UAV.

Some other researchers have focused on an infrastructure-less environment requiring a backhaul connection. In [7], the system model includes some UAVs and tethered balloons with a fiber tether cable. The backhaul links are between tethered balloons and UAVs, and the fronthaul links are between UAVs and ground users. The target is to achieve the best end-to-end throughput of the system model. So, the paper has not mentioned charging UAVs to make the model's connectivity continuous. In research [8], they categorized UAVs into three different types for specific usage. The communication drones are to communicate with all ground wireless devices in disaster-affected areas. They receive and transfer information from/to a tethered backhaul drone via FSO/RF hybrid links. However, they need another power drone to charge energy on the fly. After finishing the survey, it seems that there is not any research related to backhaul connections using UAVs while considering wireless power transfer.

Our paper contributes to the usage of UAVs for a backhauling network with concern for charging the flying UAV via FSO communication. The data transmission between UAVs is satisfied by keeping a targeted BER. The equation of harvested energy is achieved after several mathematical steps. Then, it is simplified to a closed-form format by the Gauss-Hermit method. The simulation results consider some factors, such as transmitted power, the initial position of the UAV, and the FSO link length, which can change the quantity of harvested energy.

II. SYSTEM AND CHANNEL MODEL

2.1. System model

Our system model contains two different communication types, optical fiber and FSO communications. A transmitter with a laser is placed on top of a truck to create optical signals. They are transmitted to a tethered backhaul UAV via a tethered cable. Consequently, they are received at the tethered backhaul UAV and then navigated to direct the optical beam toward the untethered UAV via FSO communication using a telescope. The FSO communication is to both transmit data and charge the untethered UAV simultaneously. The end-to-end trait from the transmitter to the untethered UAV is supported to transmit optical signals. Using optical signals ensures a high data rate for backhaul connection and a better charge for the untethered UAV.

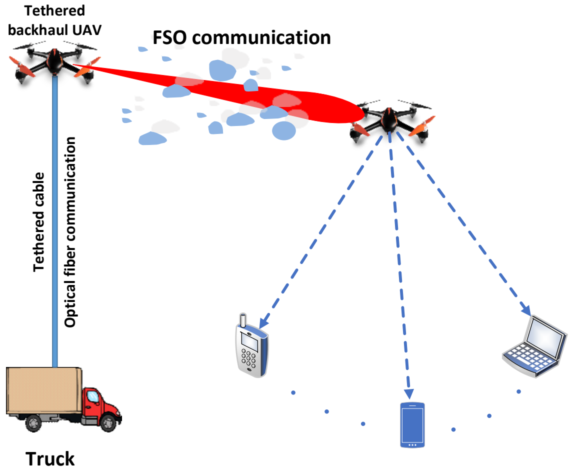

Fig 1. The tethered UAV-to-UAV model

2.2. Channel model

Our signals are transferred through a optical tethered cable firstly to reach to the tethered backhaul UAV. However, the flying height is $100m$ which nearly equals to the length of the optical tethered cable. In optical communication, the transmission loss caused by such optical cable is extremely small that we can seemingly ignore it. In the second phase, the signals are transmitted through the most struggling communication, FSO. In FSO channel, we take into account atmospheric attenuation, turbulence and pointing error. The channel state h is show in the following equation

$$h = h_l h_a h_{pe}, \tag{1}$$

where h_l, h_a and h_{pe} are represented atmospheric attenuation, turbulence and pointing error, respectively.

a. Atmospheric attenuation

Atmospheric attenuation expresses the phenomenon of energy reduction while the optical signals are transferred over a certain distance in the air. The reduction happens because gas molecules and aerosol particle naturally exiting in the air absorb the laser beam energy. So, the longer distance is, the more loss is. The Beer-Lambert law [9] describes the path loss h_l as follows

$$h_l = \exp\left(-\sigma_{air} L\right), \tag{2}$$

where L is the propagation path length of FSO link, and σ_{air} is the attenuation coefficient of the atmosphere.

$$\sigma_{air} = 10log_{10}(E_u)\frac{3.912}{V}\left(\frac{\lambda}{550}\right)^{-q(V)}, \tag{3}$$

where E_u is the Euler's constant, λ (nm) is the FSO wavelength, V (km) is the visibility, and $q(V)$ is the specific atmospheric attenuation visibility coefficient.

b. Atmospheric turbulence

Atmospheric turbulence is the spatial and temporal random fluctuation caused by some air conditions such as temperature, pressure, and wind. Those conditions cause spatial and temporal random fluctuation, so called turbulence [10]. The received irradiance, h_a, of the optical wave can be modeled as a product of small-scale, α, and large-scale, β, turbulent eddies, and its probability density function (PDF) can be expressed as

$$f_{h_a}(h_a) = \frac{2(\alpha\beta)^{\frac{\alpha+\beta}{2}}}{\Gamma(\alpha)\Gamma(\beta)} h_a^{\frac{\alpha+\beta}{2}-1} K_{\alpha-\beta}\left(2\sqrt{\alpha\beta h_a}\right), \tag{4}$$

where $\Gamma(.)$ is the gamma function and $K_v(.)$ is the v-th order modified Bessel function of the second kind. For slant FSO link propagation path, the Rytov variance, σ_R^2, is used to calculate both α and β as followed

$$\alpha = \left[exp\left(\frac{0.49\sigma_R^2}{(1+1.11\sigma_R^{12/5})^{7/6}}\right)\right]^{-1}, \tag{5}$$

$$\beta = \left[exp\left(\frac{0.51\sigma_R^2}{(1+0.69\sigma_R^{12/5})^{5/6}}\right)\right]^{-1}, \tag{6}$$

$$\sigma_R^2 = 2.25k^{7/6}[\sec(\zeta)]^{11/6}\int_{h_1}^{h_2} C_n^2(h)(h - h_1)^{5/6}dh, \tag{7}$$

where $k = 2\pi/\lambda$ is the wave number, and $C_n^2(h)$ is the refractive-index structure parameter. In [11], the Hufnagel Valley Boundary (HVB) is widely used to model $C_n^2(h)$ and can be given by

$$C_n^2(h) = 0.00594\left[\frac{w^2}{729}(10^{-5}h)^{10}exp\left(-\frac{h}{1000}\right) + 2.7\times 10^{-16}exp\left(-\frac{h}{1000}\right) + C_n^2(0)exp\left(-\frac{h}{100}\right)\right], \tag{8}$$

where w^2 is the mean square value of the wind velocity in m/s, h is the height above the surface of the earth in m, and $C_n^2(0)$ is a factor which can be adjusted to match various site conditions and given as

$$C_n^2(0) = 1.29 \times 10^{-12} r_0^{-\frac{5}{3}} \lambda^2 - 1.61 \times 10^{-13} \theta_0^{-\frac{5}{3}} \lambda^2 + 3.89 \times 10^{-15}, \tag{9}$$

where r_0 is the atmospheric coherence length and θ_0 is the isoplanatic angle. Normally, the value of the wind speed and the factor $C_n^2(0)$ is chosen as 21 (m/s) and 5×10^{-13} (m/s), respectively.

c. Pointing error model

In our system model, at the transmitter side, a telescope is mounted onto tethered UAV. Then, we assume that the vibration of the tethered UAV can be ignore. The pointing misalignment here is only from the hovering of the rotary wing UAV due to the effect of the wind. In another word, the wind will change the position of the UAV's aperture that leads to the pointing misalignment. As depicted in Fig. 2, as the UAV is flying, its initial location does not need to be in the center of the Gaussian beam footprint. In order to observe the hovering effect, the radial vectors from the beam center to the UAV's initial position, and to the UAV's actual position due to hovering are r and r_{pe}, respectively. r_h is a vector describing the hovering trait from initial to actual position. $r_{pe}(x_{pe}, y_{pe})$ can be expressed in the coordinate plane as followed

$$\begin{cases} x_{pe} = r_x + x_{r_h} = \|r\| \sin(\varphi) + x_{r_h} \\ y_{pe} = r_y + y_{r_h} = \|r\| \cos(\varphi) + y_{r_h} \end{cases}, \tag{10}$$

where x_{r_h} and y_{r_h} are zero-mean Gaussian random variables with variance σ_p^2. x_{pe} and y_{pe} are thus two statistically independent Gaussian random variables as $x_{pe} \sim N(r_x, \sigma_p^2)$ and $y_{pe} \sim N(r_y, \sigma_p^2)$. As a results, $r_{pe} = \sqrt{x_{r_{pe}}^2 + y_{r_{pe}}^2}$ is a Rice distribution with the PDF given by

$$f_{r_{pe}}(r_{pe}) = \frac{r_{pe}^2}{\sigma_p^2} \exp\left(-\frac{r_{pe}^2 + r^2}{2\sigma_p^2}\right) I_0\left(\frac{r_{pe} r}{\sigma_p^2}\right), \tag{11}$$

where I_0 is the modified Bessel function of the first kind with order zero. Let A be the area of the receiving aperture, the loss due to pointing misalignment is expressed as [12]

$$I_{pe} = \int_A I_{beam}(r - r_{pe}, L) dr \approx A_0 \exp\left(-\frac{2 r_{pe}^2}{w_{Leq}^2}\right), \tag{12}$$

where $A_0 = [\text{erf}\,(v)]^2$ is the fraction of collected power by UAV's detector at $r_{pe} = 0$. $w_{Leq}^2 = w_L^2 \frac{\sqrt{\pi}\text{erf}\,(v)}{2v\exp(-v^2)}$ is the equivalent beam width, $v = \frac{a\sqrt{\pi}}{w_L\sqrt{2}}$ in which a is the radius of the detector, $w_L \approx w_0 \sqrt{1 + \varepsilon\left(\frac{\lambda L}{\pi w_0^2}\right)^2}$ is the beam-waist at distance L, w_0 is the beam waist at the distance L = 0. The conditional PDF of I_{pe} can be expressed as

$$f_{h_{pe}}(h_{pe}) = \frac{w_{Leq}^2}{4A_0\sigma_p^2} \exp\left(-\frac{r^2}{2\sigma_p^2}\right) \left(\frac{h_{pe}}{A_0}\right)^{\frac{w_{Leq}^2}{4\sigma_p^2}} \times I_o\left(\frac{r}{\sigma_p^2}\sqrt{-\frac{w_{Leq}^2}{2}\ln\left(\frac{h_{pe}}{A_0}\right)}\right). \tag{13}$$

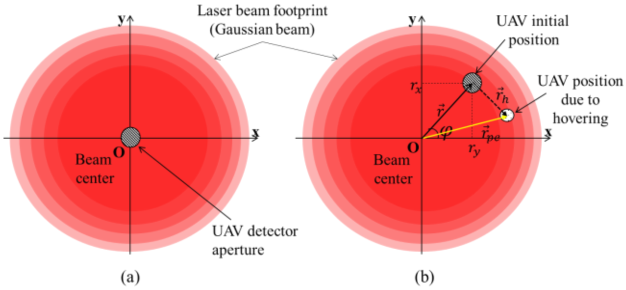

Fig. 2. Pointing error model with hovering effect

All above factors including atmospheric attenuation, turbulence-induced fading, and UAV hovering induced pointing misalignment, are modeled in a combined channel. Applying the same methodology in [13], using Gauss-Hermit quadrature and several mathematical manipulations, the closed-form of combined channel model of FSO-based tethered-UAV-to-UAV is finally derived as

$$f_h(h) = \sum_{i=1}^{N} 4x_i w_i \frac{(\alpha\beta)^{\frac{\alpha+\beta}{2}}}{\Gamma(\alpha)\Gamma(\beta)} \exp\left(-\frac{r^2}{2\sigma_p^2}\right) \left(\frac{1}{A_0 h_l}\right)^{\frac{\alpha+\beta}{2}} \times \exp\left[\frac{2x_i^2\sigma_p^2(\alpha+\beta)}{w_{Leq}^2}\right] I_0\left(\frac{r\sqrt{2}x_i}{\sigma_p}\right) \times K_{\alpha-\beta}\left(2\sqrt{\frac{\alpha\beta h}{A_0 h_l}\exp\left(\frac{4x_i^2\sigma_p^2}{w_{Leq}^2}\right)}\right) h^{\frac{\alpha+\beta}{2}-1}. \tag{14}$$

where N is the number of sample points. w_i and x_i are the weights and the zeros of Hermite polynomial, respectively.

III. DATA TRANSMISSION AND HARVESTED ENERGY

We consider the FSO-based tethered UAV-to-UAV system with the on-off keying (OOK) as the modulation scheme. The transmitted signal is given by

$$x(t) = \begin{cases} A & \text{If the bit 1 is transmitted} \\ -A & \text{If the bit 0 is transmitted} \end{cases}, \tag{15}$$

where A is the peak amplitude. Before being used to modulate the optical intensity of the laser diode (LD), a DC bias B is added to x(t) to ensure that the resulting signal is non-negative. The emitted optical signal can be written as $P_t(t) = P_{LD}[B + x(t)]$ where P_{LD} is the transmitted power. The peak amplitude A is given by

$$A = \begin{cases} B - I_L & \text{If } B < (I_L + I_H)/2 \\ I_H - B & \text{If } B \geq (I_L + I_H)/2 \end{cases}, \tag{16}$$

where I_L and I_H are the minimum and maximum input bias current, respectively.

The transmitted optical signal goes through the atmosphere propagation medium and reaches the destination. The received electrical signal can be then expressed as

$$i(t) = \mathcal{R} h P_t(t) + n(t), \tag{17}$$

where $\mathcal{R}$ is the photo-detector responsivity, and *n(t)* is the additive white Gaussian noise (AWGN) term with zero mean and variance of σ_n^2. Replacing the definition of $P_t(t)$, we have

$$\begin{aligned} i(t) &= I_{DC} + I_{AC}(t) \\ &= \mathcal{R} h S_a P_{LD} \eta B + \left(\mathcal{R} h S_a P_{LD} \xi x(t) + n(t)\right), \end{aligned} \tag{18}$$

where I_{DC} and $I_{AC}(t)$ respectively denote the DC and AC components. ξ is the optical-to-electrical conversion coefficient.

The harvested energy (conditioned on the random coefficient I) at the UAV can be written as [14]

$$E_h = \frac{1.5T_{EH}V_t(\eta h\mathcal{R}S_aP_{LD}B)^2}{I_d}, \quad (19)$$

where V_t is the thermal voltage with the typical value of 25 mVolt and I_d is the dark saturation current of solar panel. η is the optical-to-electrical conversion coefficient. S_a denotes the area of the photo-detector.

Averaging over the PDF of the combined channel, the average harvested energy can be expressed as

$$\begin{aligned}\bar{E}_h &= \int_0^\infty \frac{1.5T_{EH}V_t(\eta h\mathcal{R}S_aP_{LD}B)^2}{I_d} \\ &\times \sum_{i=1}^N 4x_iw_i\frac{(\alpha\beta)^{\frac{\alpha+\beta}{2}}}{\Gamma(\alpha)\Gamma(\beta)}\exp\left(-\frac{r^2}{2\sigma_p^2}\right)\left(\frac{1}{A_0h_l}\right)^{\frac{\alpha+\beta}{2}} \\ &\times \exp\left[\frac{2x_i^2\sigma_p^2(\alpha+\beta)}{w_{Leq}^2}\right]I_0\left(\frac{r\sqrt{2}x_i}{\sigma_p}\right) \\ &\times K_{\alpha-\beta}\left(2\sqrt{\frac{\alpha\beta h}{A_0h_l}\exp\left(\frac{4x_i^2\sigma_p^2}{w_{Leq}^2}\right)}\right)h^{\frac{\alpha+\beta}{2}-1}dh.\end{aligned} \quad (20)$$

By using the Eq. (14) and Eq. (24) in [15], after several manipulations, the closed-form of the above integral can be expressed with the help of Gauss-Hermit method.

$$\begin{aligned}\bar{E}_h &= \sum_{i=1}^N \frac{3x_iw_iT_{EH}V_t\left(\eta h\mathcal{R}A\sqrt{P_t}B\right)^2}{I_d\Gamma(\alpha)\Gamma(\beta)}\left(\frac{\alpha\beta}{A_0h_l}\right)^{\frac{\alpha+\beta}{2}} \times \\ &\exp\left[\frac{2x_i^2\sigma_p^2(\alpha+\beta)}{w_{Leq}^2}-\frac{r^2}{2\sigma_p^2}\right]I_0\left(\frac{r\sqrt{2}x_i}{\sigma_p}\right)\Gamma(\alpha+ \\ &2)\Gamma(\beta+2).\end{aligned} \quad (21)$$

In our work, we consider bit error (BER) as the performance metric for transmission fidelity. Let Ts denotes the symbol duration, the BER of OOK (conditioned on the random coefficient h) is given by

$$BER = Q\left(\sqrt{\frac{(\mathcal{R}hS_aP_{LD}A)^2T_s}{N_0}}\right). \quad (22)$$

By using the same method proposed in [16], [17], the average of energy harvesting with respect to h as shown

$$\begin{aligned}\bar{E}_h &= \sum_{i=1}^N \frac{x_iw_i}{\sqrt{\pi}}\frac{(\alpha\beta)^{\frac{\alpha+\beta}{2}}}{\Gamma(\alpha)\Gamma(\beta)}\exp\left(-\frac{r^2}{2\sigma_p^2}\right)\left(\frac{1}{A_0h_l}\right)^{\frac{\alpha+\beta}{2}} \\ &\times \exp\left[\frac{2x_i^2\sigma_p^2(\alpha+\beta)}{w_{Leq}^2}\right]I_0\left(\frac{r\sqrt{2}x_i}{\sigma_p}\right) \\ &\times \left[\frac{(\mathcal{R}S_aP_{LD}A)^2T_s}{N_0}\right]^{-\frac{\alpha+\beta}{4}} \\ &\times G_{2,3}^{2,2}\left[\frac{\frac{\alpha\beta}{A_0h_l}\exp\left(\frac{4x_i^2\sigma_p^2}{w_{Leq}^2}\right)}{\sqrt{\frac{N_0}{(\mathcal{R}S_aP_{LD}A)^2T_s}}}\middle|\begin{matrix}a_1,a_2\\ b_1,b_2,b_3\end{matrix}\right],\end{aligned} \quad (23)$$

where $a_1 = 1-\frac{\alpha+\beta}{2}$, $a_2 = \frac{1}{2}-\frac{\alpha+\beta}{2}$, $b_1 = \frac{\alpha-\beta}{2}$, $b_2 = \frac{\beta-\alpha}{2}$, $b_3 = -\frac{\alpha+\beta}{2}$ and G is Meijer-G function.

Consider a trasmission duration T_{tot}, the receiver works in ID mode for a duration of $T_{ID} = \tau T_{tot}$ with the time splitting factor τ. This corresponds to τN symbols out of N symbols. Taking a time average, the BER for the simultaneous lightwave information and power transfer (SLIPT) scheme is obtained as [18]

$$\overline{BER}_{ave} = \frac{1}{N}(\tau N)\overline{BER} = \tau\overline{BER}. \quad (24)$$

In the following, we aim to maximize the average harvested energy by proper choice of τ while satisfying a given BER target. Let BER_t denote the required maximum BER value. Mathematically speaking, we can write our optimization problem as

$$\begin{aligned}&\underbrace{max}_{\tau}\ \bar{E}_h \\ &s.t.\underbrace{\overline{BER}_{ave}}_{0\le\tau\le1} \le BER_t.\end{aligned} \quad (25)$$

The optimization problem above can be solved by choosing the minimum value of τ in the range of [0, 1] which satisfies the BER target. Noting that $T_{EH} = (1-\tau)T_{tot}$ and utilizing (23), we can obtain the optimum T_{EH} as

$$T_{EH} = \left[1-\left(\frac{BER_t}{\overline{BER}}\right)\right]T_{tot}. \quad (26)$$

IV. SIMULATION RESULTS

This section provides numerical results for the harvested energy in an FSO-based UAV system considering atmospheric attenuation, turbulence-induced fading, and UAV hovering. System parameters used in the analysis are expressed in Table I. Monte Carlo simulations using MATLAB are also provided to confirm the theoretical results.

Table 1. Simulation parameters

Parameters	Symbol	Value
Wavelength	λ	1550 nm
Tethered UAV altitude	h_1	100 m
UAV altitude	h_2	50
Wind speed	w	21 m/s
Visibility	V	30 km
Aperture radius	a	10 cm
Responsibility	$\Re$	0.8 A/W
LD power	P_{LD}	30 W/A
BER target	BER_t	10^{-6}
Symbol duration	T_s	1 μs
Power spectral density of noise	N_0	10^{-22} W/Hz
Dark saturation current of PD	I_d	10^{-9} A
Minimum input bias current	I_L	25 mA
Maximum input bias current	I_H	45 mA
Thermal voltage	V_t	25 mV

First, the harvested energy of the FSO-based Tethered UAV-to-UAV, which depends on transmitted power with different initial positions, is shown in Fig. 3. When the transmitted power increases, the harvested energy goes up. Obviously, the more transmitted energy transfers to the UAV, the more received energy collects. The initial positions of the UAV play a vital role in how much energy is harvested at the PD. When the UAV stays closer to the center of the beam, this fact leads to harvesting more energy. The reason is that transmitted energy is more intensive at the beam center. So, at a targeted harvested power and initial position of the UAV, the transmitted power can be set accordingly.

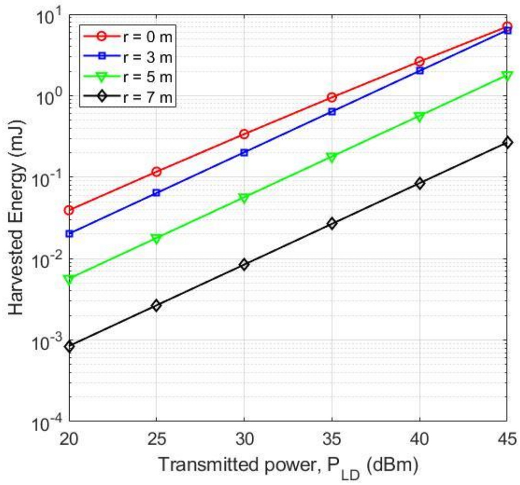

Fig. 3. Harvested energy versus the transmitted power with the FSO propagation of 500 m and beam-waist of 45 micromet.

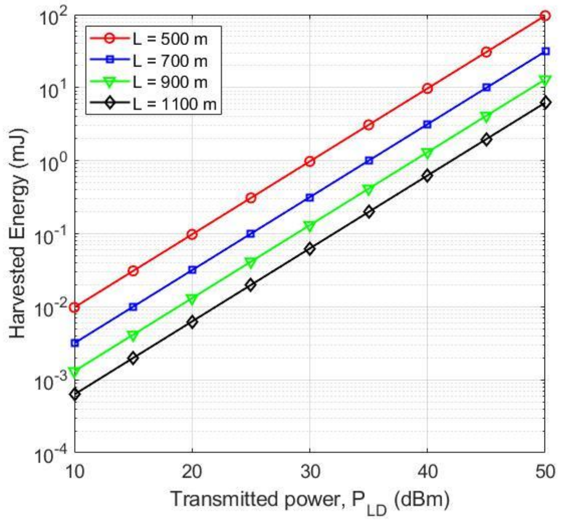

Fig. 4. The relationship between harvested energy and transmitted power in different of FSO link length with r = 1 m and w_0 = 35 micromet.

Secondly, we analyze the harvested energy with different Tethered UAV-to-UAV distances, so-called FSO link lengths in Fig. 4. At the same distance, the energy is harvested more when the power is transmitted more. L affects mainly due to atmospheric attenuation and atmospheric turbulence. The longer the distance is, the more attenuation and the less harvested energy is. Among different L values of the distances, the smallest L $500m$ always has the most energy at the same transmitted power. At $L = 500m$, when the transmitted power increases each 10 dBm, the energy gains more ten times. For example, P_{LD} is 10, 20, 30, 40, and 50 dBm, harvested energy is $0.01, 0.1, 1, 10$ and 100 mJ, respectively.

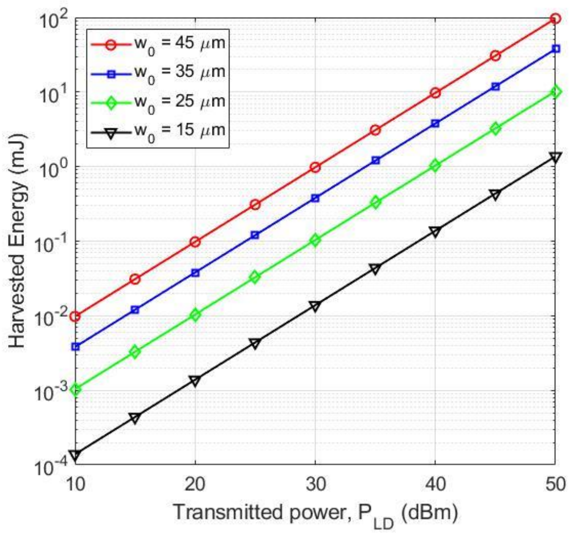

Fig. 5. The impact of beam-waist on the harvested energy over the range of transmitted power with FSO link length of 500 m and r = 1 m.

Finally, we consider the impact of beam-waist on the harvested energy over the range of transmitted power when we set $L = 500m, r = 1m$ in Fig. 5. The same pattern with four scenarios, the larger amount of energy goes along with the stronger transmitted power. However, the bigger beam-waist leads to absorbing more energy at the PD. So, comparing four lines, the line of the biggest beam-waist $w_0 = 45\mu m$ always gets the most energy.

V. CONCLUSION

A mixture model combining two UAV types, tethered UAVs and untethered UAVs, has become more powerful in providing faster backhaul connection and more effective harvested energy. In our research system, a tethered UAV connected to a truck by a cable can send fast data transmission and charge more energy to a flying UAV through an FSO link. The simulation results have shown how much some factors, such as transmitted power, the initial position of the UAV, and the FSO link length, affect the harvested energy. The FSO channel has included atmospheric attenuation, turbulence, and pointing error. The usage of a mixture model of tethered UAVs and UAVs has opened a new broad research attraction. Instead of only one link between a tethered UAV and a UAV, the network may involve several UAV links, which need to be considered more. And the FSO link can be more realistic when we can add more factors, such as the vibration or shake of tethered UAV. A new and broad road needs more researchers to engage themselves.

ACKNOWLEDGEMENT

The research was supported by APNIC foundation under The Switch! project.

REFERENCES

[1] ITU Publications, "Measuring digital development: Facts and figures," 2021. [Online]. Available: https://www.itu.int/en/ITU-D/Statistics/ Documents/facts/FactsFigures2021.pdf
[2] "3GPP UAS-UAV work items," https://www.3gpp.org/uas-uav, [Online; accessed 25-October-2020].
[3] B. Han, W. Jiang, M. A. Habibi, and H. D. Schotten, "An abstracted survey on 6G: Drivers, requirements, efforts, and enablers," 2021, arXiv:2101.01062.
[4] M. W. Akhtar, S. A. Hassan, R. Ghaffar, H. Jung, S. Garg, and M. S. Hossain, "The shift to 6G communications: Vision and requirements," Hum-Centric Comput. Inf. Sci., vol. 10, no. 1, pp. 1–27, 2020.
[5] B. E. Y. Belmekki and M. -S. Alouini, "Unleashing the Potential of Networked Tethered Flying Platforms: Prospects, Challenges, and Applications," in IEEE Open Journal of Vehicular Technology, vol. 3, pp. 278-320, 2022.
[6] Y. L. Che, W. Long, S. Luo, K. Wu, and R. Zhang, "Energy-efficient uav multicasting with simultaneous fso backhaul and power transfer," IEEE Wireless Communications Letters, vol. 10, no. 7, pp. 1537 -1541, 2021.
[7] A. Alzidaneen, A. Alsharoa and M. -S. Alouini, "Resource and Placement Optimization for Multiple UAVs using Backhaul Tethered Balloons," in IEEE Wireless Communications Letters, vol. 9, no. 4, pp. 543-547, April 2020.
[8] M. Y. Selim and A. E. Kamal, "Post-Disaster 4G/5G Network Rehabilitation Using Drones: Solving Battery and Backhaul Issues," 2018 IEEE Globecom Workshops (GC Wkshps), 2018, pp. 1-6.
[9] T. V. Nguyen, T. V. Pham, N. T. Dang, and A. T. Pham, "Performance of generalized qam/fso systems with pointing misalignment and phase error over atmospheric turbulence channels," IEEE Access, vol. 8, pp. 203631– 203644, 2020.
[10] A. C. Motlagh, V. Ahmadi, Z. Ghassemlooy, and K. Abedi, "The effect of atmospheric turbulence on the performance of the free space optical communications," in 2008 6th International Symposium on Communication Systems, Networks, and Digital Signal Processing, pp. 540–543, 2008
[11] H. Kaushal and G. Kaddoum, "Optical communication in space: Challenges and mitigation techniques," IEEE Commun. Surveys Tuts., vol. 19, pp. 57–96, First quarter 2017.
[12] A. A. Farid and S. Hranilovic, "Outage capacity optimization for free-space optical links with pointing errors," J. Lightw. Technol., vol. 25, pp. 1702–1710, July 2007.
[13] T. V. Nguyen, T. V. Pham, N. T. Dang, and A. T. Pham, "Uav-based fso systems using sc-qam signaling over fading channels with misalignment," in 2020 IEEE 92nd Vehicular Technology Conference (VTC2020-Fall), pp. 1–5, 2020.
[14] J. Chen, L. Yang, W. Wang, H.-C. Yang, Y. Liu, M. O. Hasna, and M.-S. Alouini, "A novel energy harvesting scheme for mixed fso-rf relaying systems," IEEE Transactions on Vehicular Technology, vol. 68, no. 8, pp. 8259–8263, 2019.
[15] V. Adamchik and O. Marichev, "The algorithm for calculating integrals of hyperfeometric type functions and its realization in reduce system," in Proc. Int. Conf. Symb. Algebraic Comput., pp. 212–224, 1990.
[16] T. V. Nguyen, H. D. Le, N. T. Dang, and A. T. Pham, "On the design of rate adaptation for relay-assisted satellite hybrid fso/rf systems," IEEE Photonics Journal, vol. 14, no. 1, pp. 1–11, 2022.
[17] Thang V. Nguyen, Hoang D. Le, and Anh T. Pham, "On the Design of RIS-UAV Relay-Assisted Hybrid FSO/RF Satellite-Aerial-Ground Integrated Network," IEEE Transactions on Aerospace and Electronic Systems, pp. 1 - 15, Jul. 2022.
[18] H. G. Sandalidis, A. Vavoulas, T. A. Tsiftsis, and N. Vaiopoulos, "Illumination, data transmission, and energy harvesting: the threefold advantage of vlc," Appl. Opt., vol. 56, pp. 3421–3427, Apr 2017.

THU THẬP NĂNG LƯỢNG GIỮA CÁC UAV CHO KẾT NỐI BACKHAUL

Tóm tắt- UAV (Phương tiện bay không người lái) trở thành một phần thiết yếu trong 6G. Các UAV giúp tạo ra kết nối trực xạ LOS dễ dàng hơn và triển khai mạng nhanh hơn. Tuy nhiên việc cung cấp kết nối backhaul và sự giới hạn về năng lượng là hai nguyên nhân chính làm chậm việc sử dụng UAV. Trong nghiên cứu này, chúng tôi đưa ra một mô hình kết hợp gồm một UAV nối dây và một UAV thông thường. UAV nối dây được nối với một xe tải bởi sợi cáp quang để có thể đảm bảo năng lượng và truyền dẫn dữ liệu tốc độ cao tới nó thông qua truyền thông quang. Sau đó, UAV nối dây này chuyển tiếp tín hiệu laze từ xe tải đến UAV để sạc và truyền dữ liệu cùng một lúc thông qua truyền thông quang không dây FSO. Chúng tôi xem xét năng lượng thu thập được tại UAV này với một BER yêu cầu cho trước. Năng lượng thu thập được đánh giá bởi nhiều yếu tố như công suất phát, vị trí của UAV và khoảng cách đường FSO trong phần mô phỏng. Kênh FSO khảo sát bởi nhiều hiện tượng ảnh hưởng như suy hao khí quyển, nhiễu loạn khí quyển và lỗi lệch hướng.

Từ khóa- Thu thập năng lượng, UAV, UAV nối dây, truyền thông FSO.

Le Tung Hoa received B.E. from Posts and Telecommunications Institute of Technology (PTIT), Vietnam, in 2007, and M.E. degree from University of Electro-communication, Japan, in 2010, both in telecommunication engineering. Now, she is a lecturer at Faculty Telecommunication 1 of PTIT. Her research interests include wireless communications, VANET, Vehicular VLC and FSO communications.

Nguyen Van Thang received B.E. from Posts and Telecommunications Institute of Technology (PTIT), Vietnam, in 2017. He obtained M.E. and Ph.D. degrees in Computer Science and Engineering from the University of Aizu (Japan) in 2019 and 2022, respectively. Now, he is a lecturer at Faculty Telecommunication 1 of PTIT. His current research interests include the aera of communication theory with a particular emphasis on modeling, design and performance analysis of hybrid FSO/RF systems, optical wireless communications, satellite communications. He is a member of IEEE.

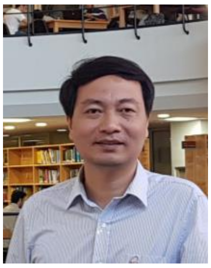

Dang The Ngoc received the Ph.D. degree in computer science and engineering from the University of Aizu (Japan). He is currently is Associate Professor/Vice Dean of Faculty of Telecommunications and Head with the Department of Wireless Communications at Posts and Telecommunications Institute of Technology (PTIT). Dr. Ngoc was also an invited researcher/ research fellow at Universite de Rennes 1, (France), the University of Seville (Spain), and the University of Aizu. His current research interests include the area of communication theory with a particular emphasis on modeling, design, and performance evaluation of optical CDMA, RoF, QKD, and optical wireless communication systems. He is a member of IEEE.